Received: 2 February 2022 | Revised: 18 March 2022 | Accepted: 19 March 2022

DOI: 10.1002/elps.202200025

ELECTROPHORESIS

RESEARCH ARTICLE

Dead volume–free flow splitting in capillary electrophoresis

Daniel Böhm | **Martin Koall** | **Frank-Michael Matysik**

Institute of Analytical Chemistry, Chemo- and Biosensors, University of Regensburg, Regensburg, Germany

Correspondence
Frank-Michael Matysik, Institute of Analytical Chemistry, Chemo- and Biosensors, University of Regensburg, Universitätsstraße 31, 93053 Regensburg, Germany.
Email: frank-michael.matysik@chemie.uni-regensburg.de

Color online: See article online to view Figures 1–5 in color.

Funding information
Deutsche Forschungsgemeinschaft, Grant/Award Number: MA1491/12-1

Abstract

In recent years, several dual detection concepts (DDCs) for CE were developed, which consisted of at least one nondestructive detector. For these DDCs, a linear detector arrangement could be used, which is not possible when both detectors are destructive. To overcome this problem, we developed a concept for the splitting of the CE stream utilizing commercially available flow splitters (FSs) that allow the parallel positioning of two destructive detectors. In this proof-of-concept study, T- and Y-shaped FSs were characterized regarding their suitability for DDCs. To keep it simple, a UV detector (UV) and a C^4D were used for the characterization. The model system consisted of an acetonitrile-based background electrolyte and the two model substances, (ferrocenylmethyl)trimethylammonium iodide and caffeine. CE hyphenated to a UV detector (CE-UV) measurements revealed that the split ratio was about 50% for both FSs. CE-C^4D was used to evaluate the peak shape in front of and behind the FSs. These measurements showed that there was no significant peak broadening introduced by the FSs. Additionally, there were no changes in the LODs in front of and behind the FSs. Furthermore, the flexibility of the new FS approach allowed the usage of capillaries with different ids (25–75 µm) for injection and detection.

KEYWORDS
capillary electrophoresis, dead volume–free, dual detection, flow splitting, various capillaries inside diameter

1 | INTRODUCTION

There is a need for powerful analytical methods as the number of samples, the sample complexity, and the amount of substances that need to be analyzed is steadily increasing [1]. In recent years, CE was established as a potent separation technique due to its high separation efficiency, the simplicity of the instrumental setup, the small sample and reagent consumption, and its high separation speed [2–5]. An ongoing trend is also the coupling of a separation technique like CE with more than one detector. These dual detection concepts (DDCs) are especially interesting when both detectors provide

Abbreviations: AD, amperometric detector; Caf, caffeine; CE-UV, CE hyphenated to a UV detector; DDC, dual detection concept; $[FcMTMA]^+$, (ferrocenylmethyl)trimethylammonium ion; FS, flow splitter; FST, T-shaped FS; FST rev., T-shaped FS reversed; FSY, Y-shaped FS; TPN, theoretical plate number.

complementary information [1, 6]. There are several DDCs for CE described in the literature [7–12]. Most DDCs consist of at least one nondestructive detector that allows a serial detector arrangement [6]. However, some analytical problems would require a combination of two destructive detectors. To our knowledge, such a DDC was not realized so far as a linear detector arrangement is not possible. One of these DDCs would be the combination of an amperometric detector (AD) and an MS. This is a very powerful DDC, because the AD is one of the most sensitive detection methods for electroactive analytes and therefore ideal for the quantification of low concentrations, whereas MS is perfect for the identification of substances [7, 13, 14]. Another interesting DDC that was also not realized so far is the combination of ESI MS and ICP MS. Karst and coworkers [15] already described the potential of CE hyphenated to both techniques but have not linked the methods with each other. The instrumental implementation of these DDCs is complicated as both detectors are destructive. To overcome these problems, we introduced a new concept for the development of DDCs consisting of two destructive detectors by splitting the CE stream utilizing commercially available flow splitters (FSs). With this approach, it would be possible to place the detectors in parallel to each other. For some applications, it is challenging to find the best suitable capillary id, due to the different requirements of injection, separation, and detection [16]. For trace analysis capillaries with bigger ids at the injection side are favorable to achieve higher sample loads. Additionally, for DDCs, the detectors could have different requirements concerning the capillary id. Due to the flexibility of the FS approach, the ids of the capillaries could be adjusted individually to the requirements of injection and of each detector. However, capillary combinations with different ids could also be used for generating higher electrical field strengths [17]. The splitting of the CE flow is already described in the literature, but this was predominately in the context of 2D separations or for the concurrent analysis of cations and anions [18–20]. In the frame of this contribution, we describe the splitting of the CE stream for the usage in DDCs. Special attention was paid to a low dead volume, easy handling, and the material of the FSs. During the project, we characterized two commercially available FSs (Y- and T-shaped) regarding their suitability for DDCs. As in a future project, it is planned to develop a novel DDC consisting of an AD and an MS, an acetonitrile (ACN)-based background electrolyte (BGE) was used, which is favorable for both detectors (AD and MS) [21, 22]. To keep it simple, CE hyphenated to a UV detector (CE-UV) and CE hyphenated to C^4D (CE-C^4D) were utilized for the characterization of the FSs.

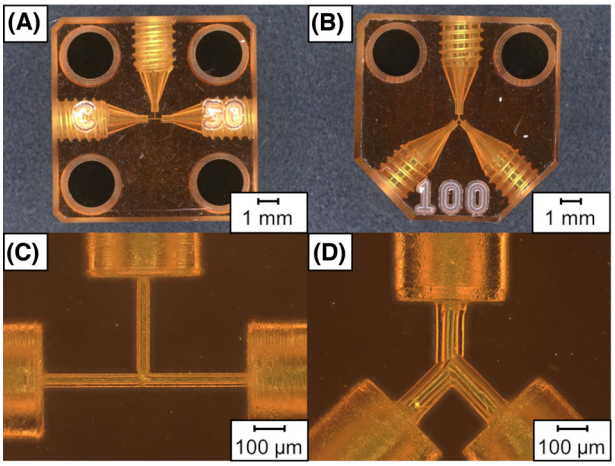

FIGURE 1 Microscope images of FST (A), FSY (B), and the corresponding close-up images of FST (C) and FSY (D). FS, flow splitter; FST, T-shaped FS; FSY, Y-shaped FS

2 | MATERIALS AND METHODS

2.1 | Chemicals, materials, and samples

The following chemicals of analytical grade were used: ACN, ammonium acetate, 0.1 M sodium hydroxide solution, and ultrapure water (Milli Q Advantage A10 system) were obtained from Merck (Darmstadt, Germany). Acetic acid was purchased from Carl Roth (Karlsruhe, Germany). (Ferrocenylmethyl)trimethylammonium iodide was bought from Strem Chemicals (Newburyport, USA). Caffeine (Caf) was obtained from ABCR (Karlsruhe, Germany). Fused silica capillaries (25, 50 and 75 µm id, 365 µm od; polyimide- and Teflon-coated) were purchased from Polymicro Technologies (Phoenix, USA). The FSs CapTite Interconnect T C360 203U C050 (FST), CapTite Interconnect Y C360 203Y (FSY) and the corresponding fitting CapTite One-Piece Fitting C360-100 were purchased from LabSmith (Livermore, USA).

All experiments (CE-UV and CE-C^4D) were performed with a nonaqueous BGE consisting of 10 mM ammonium acetate and 1 M acetic acid in ACN. The sample solution for the CE-UV experiments consisted of 0.5 mM ferrocenylmethyl)trimethylammonium ion ($[FcMTMA]^+$) and Caf in BGE. For the CE-C^4D experiments, the sample solutions consisted of 0.1 mM $[FcMTMA]^+$ in BGE. The data analysis was performed with OriginPro 2020 (Northampton, USA).

2.2 | Properties of the FSs and capillary preparation

The two commercially available FSs, which were used in this project, are shown in Figure 1. The T-shaped FS (FST,

Figure 1A and C) had a thru-hole diameter of 50 µm, which resulted in a dead volume of 2.1 ± 0.5 nl. According to technical reasons the Y-shaped FS (FSY, Figure 1B and D) had a thru-hole diameter of 100 µm, which resulted in a dead volume of 9 ± 2 nl. Both the FSs were, fabricated from polyetherimide, also known by the trade name Ultem. The FSs did not show any swelling or other visual changes when they came into contact with the ACN-based BGE. Capillaries were connected to the FSs with commercially available fittings, which were suitable for 365 µm od capillaries. These fittings were fabricated from polyether ether ketone and were therefore also resistant against ACN.

Three capillary pieces were connected to the FS, a 20 cm long capillary piece was assembled to the injection side (P1) of the FS. At the two other sides of the FS (detection sides, P2 and P3), capillary pieces with a length of 40 cm were placed. To avoid any dead volume introduced by polyimide swelling, about 2 mm of the outer polymer coating of the capillary was removed. Additionally, both sides of each capillary were polished to receive planar capillary tips that enable a dead volume–free coupling with the FS. Before the first CE measurements, the capillaries were conditioned by flushing with 0.1 M sodium hydroxide solution (10 min), ultrapure water (5 min), and finally BGE (30 min).

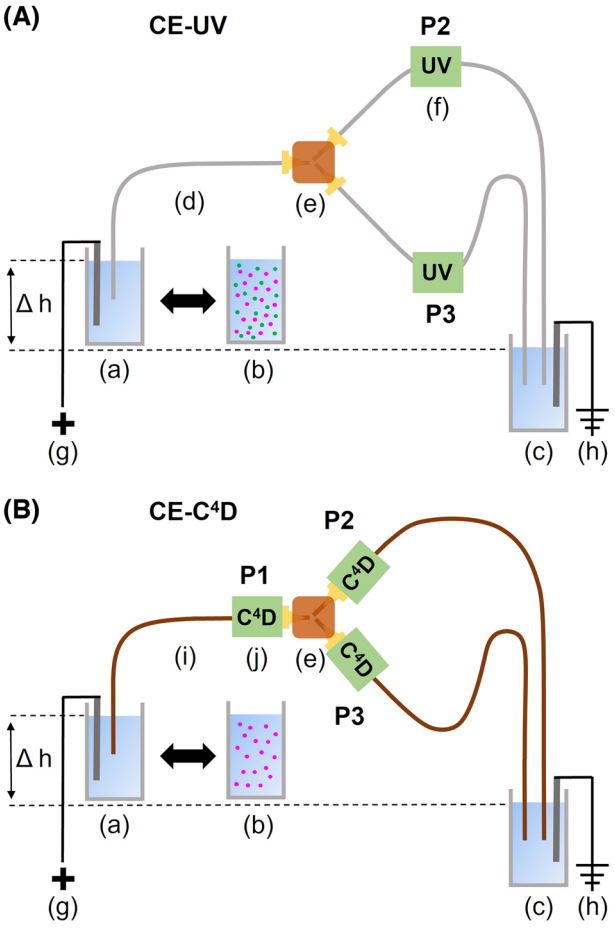

FIGURE 2 Scheme of the CE-UV setup (A) and the CE-C^4D setup (B). Components of the CE-UV setup: inlet (a), sample (b), and outlet BGE vial (c), Teflon-coated fused silica capillaries (d), FST or FSY (e), UV detector (f), positive high voltage source (g), and grounding (h). Components of the CE-C^4D setup: polyimide-coated fused silica capillaries (i) and C^4D (j). For both setups, there was a permanent height difference between the injection and detection side of 15 cm. The position of the detectors (UV and C^4D) was changed without disassembling the capillary pieces from the FS. BGE, background electrolyte; CE-UV, CE hyphenated to a UV detector; FS, flow splitter; FST, T-shaped FS; FSY, Y-shaped FS

2.3 | CE-UV setup

Figure 2A shows a scheme of the CE-UV setup. It consisted of a laboratory-constructed CE device with an integrated autosampler that was connected to a positive high-voltage power supply from ISEG (Radeberg, Germany). Experiments were carried out with FST and FSY. Each FS was connected to three capillaries (50 µm id and 365 µm od). Both capillary ends were placed in a grounded outlet vial. There was a permanent height difference between the inlet and outlet vials of 15 cm. The injection was performed hydrodynamically for 5 s. The UV detector was placed after a capillary length of 40 cm (20 cm behind the FS). A Lambda 1010 UV–VIS detector from Bischoff (Leonberg, Germany) was used for detection at 265 nm. For calculating the split ratio and other parameters, measurement data were needed for both detection sides behind the FS (P2 and P3, highlighted in Figure 2A). As only one UV detector was available, a simultaneous detection at both sides (P2 and P3) was not possible. Therefore, the position of the UV detector was changed between P2 and P3. To minimize potential errors, during the position change of the detector, the capillary pieces were not disassembled from the FS. Thus, for each set of measurements, there was the same capillary to FS alignment, because only the position of the detector was swapped. To simplify the detector change, Teflon-coated capillaries were used. Due to the transparent Teflon coating, no coating must be removed at the detection point of the UV detector, which makes the capillary less brittle. Five consecutive measurements were performed at P2 and P3. The sample solution consisted of 0.5 mM $[FcMTMA]^+$ as a cationic model analyte and 0.5 mM Caf as an EOF marker. The separations were performed at 25 kV. Special attention is needed when experiments are performed with high voltage. Hence, the whole setup was placed in a safety housing made of acrylic glass. Additionally, the device was equipped with safety switches and warning signs.

2.4 | CE-C^{4}D setup

CE-C^{4}D was used to evaluate the peak shape in front of and behind the FS. The CE-C^{4}D setup is depicted in Figure 2B. For detection, a C^{4}D was used, which was constructed in the group of Prof. C. L. do Lago and is described elsewhere [23]. Due to its compact design, the C^{4}D could be placed directly in front of (P1) and behind the FSs (P2 and P3). The detector positions are highlighted in Figure 2B. As described for the CE-UV setup, the position of the C^{4}D was changed after five measurements without disassembling the capillary pieces from the FSs. Experiments were carried out with FST and FSY. In contrast to the CE-UV setup, capillaries (50 µm id and 365 µm od) with polyimide coating were used. The sample solution consisted of 0.1 mM [FcMTMA]$^+$ in BGE. The other parameters were identical to the CE-UV setup.

The LODs were determined in front of (P1) and behind FSY (P2). Sample solutions ranging from 0.01 to 0.25 mM [FcMTMA]$^+$ in BGE were used. Each measurement was performed five times and the LODs were calculated for an S/N of 3. The effect of different FS geometries was investigated by measurements with a reversed FST (FST rev.). In this case, the injection capillary (P1) and one outlet capillary (P2) were arranged linearly, whereas the other outlet capillary (P3) was arranged perpendicularly.

To achieve higher sample loads and to show the flexibility of the FSs regarding different capillary IDs, FSY was connected at P1 with two capillary pieces of different ids (50 and 75 µm). At P2 and P3, there were still capillaries with an id of 50 µm. To compare the effects, we injected a sample plug of the same length (2.8 mm) in each capillary combination. The corresponding injection times were calculated based on capillary flow injection experiments. The injection of the sample solution (0.1 mM [FcMTMA]$^+$ in BGE) was performed hydrodynamically by a height difference of 10 cm between the inlet and outlet BGE vials. During the electrophoretic separation, the BGE levels in the vials were at the same height to avoid gravity-driven flow. For each capillary combination, the detector was placed at P1, P2, and P3.

3 | RESULTS AND DISCUSSION

3.1 | Characterization of the FSs

As the FS would be the central component for the realization of new DDCs, it must fulfill certain requirements: (i) The FS should have a low dead volume to prevent peak broadening or mixing of already separated analyte zones. (ii) The material of the FS should be resistant against organic solvents especially ACN, because we used an ACN-based BGE. (iii) The connection of the capillaries to the FS should be easy, robust, and flexible.

We chose commercially available FSs (FST and FSY, depicted in Figure 1) instead of expensive and time-consuming laboratory-constructed FSs. Both the FSs used fulfill the abovementioned requirements. Additionally, the transparency of the material simplified the troubleshooting as air bubbles inside the FS can be easily recognized. As they were commercially available, they also showed very good reproducibility contrary to laboratory-constructed items.

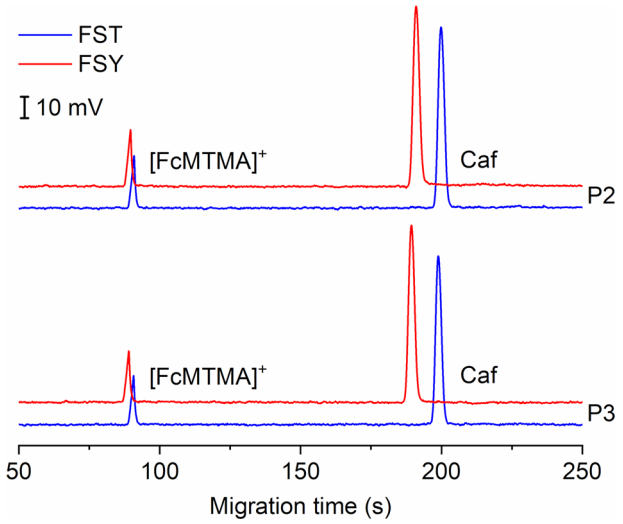

FIGURE 3 Electropherograms of the model mixture [FcMTMA]$^+$/Caf were measured with CE-UV. The UV detector was placed at P2 (top) and P3 (bottom) of FST and FSY. Experimental parameters: 0.5 mM [FcMTMA]$^+$ and Caf in BGE, injection time 5 s, separation voltage 25 kV, current 6.7 µA (FST), and 6.9 µA (FSY), UV detection at 265 nm. The UV detector was placed after a capillary length of 40 cm (20 cm behind the FS). BGE, background electrolyte; Caf, caffeine; CE-UV, CE hyphenated to a UV detector; [FcMTMA]$^+$, (ferrocenylmethyl)trimethylammonium ion; FS, flow splitter; FST, T-shaped FS; FSY, Y-shaped FS

3.2 | Characterization of the FSs utilizing UV detection

The electropherograms for FST and FSY with parallel UV detection at different sides (P2 and P3) are depicted in Figure 3. The measurements showed that the splitting of the CE flow with the FSs worked because the model analytes were detected at both capillary sides. Looking at the peak shape, it was found that all peaks showed nearly Gaussian shape with negligible peak tailing for both FSs. For the development of new DDCs, the split ratio and its

reproducibility are of special importance. The parameters were calculated based on the peak areas of the cationic and neutral model analytes at both sides (P2 and P3) and are summarized in Table S1. For FST, the split ratio was a little closer to 50% than for FSY, but the reproducibility of the splitting was better for FSY. In our opinion, the reproducibility of the splitting is more important than the split ratio because it is mandatory for the reliable quantification of the analytes that the split ratio is stable throughout the measurements. The theoretical plate numbers (summarized in Table S1) were slightly higher for FST, which indicated better separation efficiency due to the smaller dead volume of FST. For both FSs, the migration times were approximately the same at both capillary sides (P2 and P3). Slight differences were only found between the FSs. For FST, the cationic model analyte ($[FcMTMA]^+$) migrated 2 s and the EOF marker (Caf) 9 s later than for FSY. The reproducibility of the migration times was better for FSY than for FST. We think this resulted from disturbances of the CE flow at the connection side between FST and the capillary pieces. For FST, the thru-hole diameter was 50 µm that was also the id of the capillary pieces. Consequently, slight shifts at the connection side could influence the CE flow, which affected the migration times. This phenomenon was intensively discussed in some of our previous works, where we coupled capillaries with different ids linearly [16]. For FSY, the robustness of the connection was better due to the thru-hole diameter of 100 µm.

From the CE experiments with parallel UV detection, one can conclude that the separation efficiency was slightly better for FST, but the reproducibility of the splitting and the robustness of the capillary coupling to the FS were better for FSY.

3.3 | Characterization of the FSs utilizing C^4D detection

The effects of the flow splitting on the peak shape were characterized by CE-C^4D. Due to its compact design, the C^4D could be placed directly in front of (P1) and behind the FS (P2 and P3). The corresponding electropherograms of the different FSs are depicted in Figure 4. The investigated sample solution consisted only of the cationic model analyte ($[FcMTMA]^+$) due to the detection characteristics of the C^4D. As observed for the CE-UV experiments, the cationic model analyte ($[FcMTMA]^+$) migrated at each side (P2 and P3) nearly simultaneously. From the electropherograms shown in Figure 4, we found that for both types of FSs, the peaks look almost identical in front of and behind the FS. The corresponding figures of merit for the peaks at P1, P2, and P3 are summarized in Table S2. It was found that the FWHMs were the same for FSY at P1, P2, and P3. The FWHMs of the peaks for FST were slightly larger behind the FS (P2 and P3). We suggest that this was also a disturbance effect from the connection side. Nevertheless, the FWHMs were almost the same in front of and behind both FSs. The sample zones were split simultaneously inside of the FS without dilution effects. Therefore, the sample zones have only half of the length after the splitting, but the peak width behind the FS was almost identical to the peak width in front of the FS. A possible explanation for the very similar peak widths could be given by the different flow rates in front of and behind the FS. We calculated the flow rates for the different sections of the FSs based on the migration times and the positions of the detectors. For FST, we determined a flow rate of 6.21 ± 0.06 mm/s at P1, 3.00 ± 0.04 mm/s at P2, and 3.1 ± 0.1 mm/s at P3. Very similar results were obtained for the flow rate of FSY. For both FSs, the flow rates prior to the FS were about twice as high as the flow rates afterward. Thus, after passing the FS the sample zones needed twice the time to pass the detector. Compared to the peak widths in front of the FS, the combination of halved sample zones and halved flow rates behind the FS leads to nearly identical peak widths behind the FS. As the sample zones were not diluted during the splitting process and the fact that the C^4D is a concentration-related detector, also the

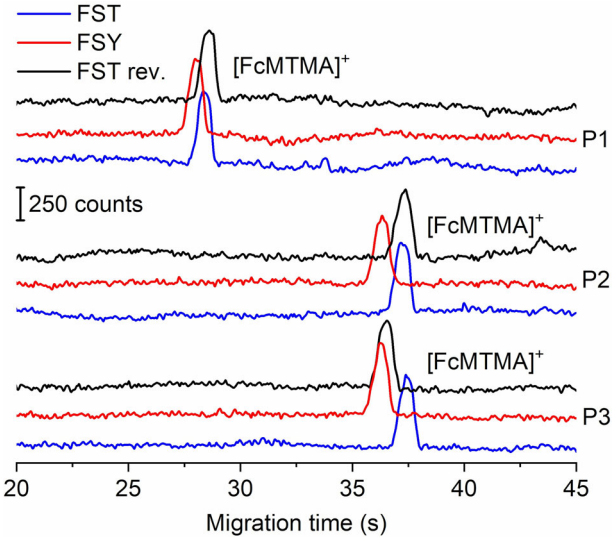

FIGURE 4 CE-C^4D measurements of FST, FSY, and FST rev. In contrast to FST for FST rev., the inlet capillary (P1) and one outlet capillary (P2) were arranged linearly, and the second outlet capillary (P3) was arranged perpendicular to them. The C^4D was placed directly in front of (P1) and behind the FSs (P2 and P3). Experimental parameters: 0.1 mM $[FcMTMA]^+$ in BGE, injection time 5 s, separation voltage 25 kV, current 6.0 µA (FST), 6.1 µA (FSY), and 6.1 µA (FST rev.). BGE, background electrolyte; $[FcMTMA]^+$, (ferrocenylmethyl)trimethylammonium ion; FS, flow splitter; FST, T-shaped FS; FSY, Y-shaped FS; FST rev., FST reversed

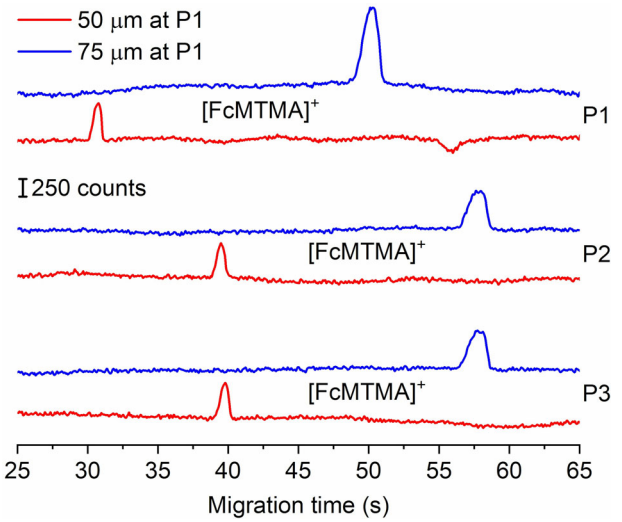

FIGURE 5 CE-C^4D measurements of an $[FcMTMA]^+$ sample solution with a 50 and 75 µm capillary in front of FSY (P1) and two 50 µm capillaries behind the FSY (P2 and P3). The C^4D was placed directly in front of (P1) and behind the FS (P2 and P3). Experimental parameters: 0.1 mM $[FcMTMA]^+$ in BGE, separation voltage 25 kV, current 6.2 µA (50 µm at P1), and 9.0 µA (75 µm at P1), sample plug length 2.8 mm. The sample plug length was calculated based on capillary flow injection experiments. BGE, background electrolyte; $[FcMTMA]^+$, (ferrocenylmethyl)trimethylammonium ion; FS, flow splitter; FSY, Y-shaped FS

peak heights were identical in front of and behind the FS. As the peaks looked nearly the same in front of and behind the FS, also the LODs should be the same. Therefore, we determined the LODs in front of and behind FSY and we found that the LODs were 13 ± 6 µM in front of the FS and 15 ± 8 µM behind the FS. Within the scope of measurement precision, the LODs could be considered identical. As our experiments did not reveal any peak broadening effects introduced by the FSs, we consider the splitting as nearly dead volume free.

As FST and FSY had different thru-hole diameters, we investigated the effect on the geometry of the FS by changing the direction of FST, so that P1 and P2 were arranged linearly. However, the other outlet capillary (P3) was arranged perpendicular to P1 and P2. The corresponding electropherograms of the reversed FST are also depicted in Figure 4. For both arrangements of FST, no significant difference was detectable. Hence, we concluded that the geometry of the FS had no measurable effect on the splitting of the CE flow.

For trace analysis, usually larger sample amounts are required. To achieve higher sample loads, by similar sample plug length, we placed a 75 µm instead of a 50 µm capillary in front of FSY (P1). Figure 5 shows the corresponding electropherograms with a 50 and 75 µm capillary at P1 for identical sample plug lengths. For the measurements using a 75 µm capillary at P1, the cationic model substance migrated at P1 20 s later compared to the configuration using the 50 µm capillary, which could be explained by the smaller electrical field strength in the 75 µm capillary. The plateau formation of the peaks at P2 and P3 for the confirmation with the 75 µm capillary approved the higher amount of injected sample compared to the configuration using the 50 µm capillary at P1. Furthermore, the peaks recorded using the 75 µm capillary at P1 were about twice as high as in the 50 µm capillary. This was predominantly an effect of the higher sensitivity of the C^4D for capillaries with a larger id and not due to the higher sample volume. Table S3 depicts the dependence of the sensitivity of the C^4D on the id of the capillary for our used model system. The data in Table S3 show that the sensitivity of the C^4D was about twice as high for the 75 µm than for the 50 µm capillary. Overall, these measurements showed the flexibility of the FS concept regarding different capillary ids and were not limited to the injection position (P1). At P2 and P3, also capillaries with different ids could be used, which allows the individual adjustment of the capillary id to the requirements of injection and of each detector.

4 | CONCLUDING REMARKS

For the development of novel DDCs, including more than one destructive detector at the capillary end, we have introduced a simple concept for the splitting of the CE stream utilizing commercially available FSs. With this approach, it was possible to place two detectors in parallel to each other.

In this manuscript, we performed some proof-of-concept experiments where we could show that the splitting of the CE flow with commercially available FSs is promising for detection concepts using two destructive detectors. Both FSs provided very good performance. Additionally, they were very simple in handling and user-friendly. The split ratio was about 50% for both types of FSs. We found that it was favorable for the reproducibility of the measurements when the thru-hole diameter of the FS was 50 µm larger than the id of the capillary. CE-C^4D measurements showed no significant peak broadening due to the implementation of the FSs. Additionally, the LODs in front of and behind the FS were the same. Consequently, the splitting can be considered almost dead volume free. Additionally, we found that the shape of the FS had no measurable effect on the splitting. The FSs were also successfully tested in combination with capillaries of various ids. Therefore, it was possible to choose the best suitable capillary id for injection and each detector individually. In contrast to conventional

DDCs with a linear detector arrangement, the concept with the FSs has, in combination with capillaries of identical ids, the potential to synchronize the detector responses.

Based on the results described in this article, it can be pointed out that utilizing commercially available FSs, the concept of CE flow splitting is a powerful and simple approach that could be used for the implementation of novel DDCs consisting of two destructive detectors. Moreover, the FSs hold great potential to be used in other, more sophisticated applications of capillary-based analytical systems.

ACKNOWLEDGMENTS

We are grateful to the Deutsche Forschungsgemeinschaft (DFG, German research foundation) for financial support (project number MA1491/12-1).

Open access funding enabled and organized by Projekt DEAL.

CONFLICT OF INTEREST

The authors have declared no conflict of interest.

DATA AVAILABILITY STATEMENT

The data that support the findings of this study are available from the corresponding author upon reasonable request.

ORCID

Frank-Michael Matysik https://orcid.org/0000-0001-7029-1382

REFERENCES

1. Beutner A, Herl T, Matysik F-M. Selectivity enhancement in capillary electrophoresis by means of two-dimensional separation or dual detection concepts. Anal Chim Acta. 2019;1057:18–35.
2. Furter JS, Boillat M-A, Hauser PC. Low-cost automated capillary electrophoresis instrument assembled from commercially available parts. Electrophoresis. 2020;41:2075–82.
3. Holland LA, Chetwyn NP, Perkins MD, Lunte SM. Capillary electrophoresis in pharmaceutical analysis. Pharm Res. 1997;14:372–87.
4. Ramos-Payán M, Ocaña-Gonzalez JA, Fernández-Torres RM, Llobera A, Bello-López MÁ. Recent trends in capillary electrophoresis for complex samples analysis: a review. Electrophoresis. 2018;39:111–25.
5. Voeten RLC, Ventouri IK, Haselberg R, Somsen GW. Capillary electrophoresis: trends and recent advances. Anal Chem. 2018;90:1464–81.
6. Opekar F, Stulík K. Some important combinations of detection techniques for electrophoresis in capillaries and on chips with emphasis on electrochemical principles. Electrophoresis. 2011;32:795–810.
7. Beutner A, Scherer B, Matysik F-M. Dual detection for non-aqueous capillary electrophoresis combining contactless conductivity detection and mass spectrometry. Talanta. 2018;183:33–8.
8. Francisco KJM, do Lago CL. A capillary electrophoresis system with dual capacitively coupled contactless conductivity detection and electrospray ionization tandem mass spectrometry. Electrophoresis. 2016;37:1718–24.
9. Mironov GG, Clouthier CM, Akbar A, Keillor JW, Berezovski MV. Simultaneous analysis of enzyme structure and activity by kinetic capillary electrophoresis-MS. Nat Chem Biol. 2016;12:918–22.
10. Szarka M, Szigeti M, Guttman A. Imaging laser-induced fluorescence detection at the Taylor cone of electrospray ionization mass spectrometry. Anal Chem. 2019;91:7738–43.
11. Zhang D, Li W, Zhang J, Tang W, Qian C, Feng M, et al. Study on urinary metabolic profile of phenylketonuria by micellar electrokinetic capillary chromatography with dual electrochemical detection–potential clinical application in fast diagnosis of phenylketonuria. Anal Chim Acta. 2011;694:61–6.
12. Huhn C, Ruhaak LR, Mannhardt J, Wuhrer M, Neusüß C, Deelder AM, et al. Alignment of laser-induced fluorescence and mass spectrometric detection traces using electrophoretic mobility scaling in CE-LIF-MS of labeled N-glycans. Electrophoresis. 2012;33:563–6.
13. Holland LA, Lunte SM. Capillary electrophoresis coupled to electrochemical detection: a review of recent advances. Anal Commun. 1998;35:1–4.
14. Matysik F-M. End-column electrochemical detection for capillary electrophoresis. Electroanalysis. 2000;12:1349–55.
15. Meermann B, Bartel M, Scheffer A, Trümpler S, Karst U. Capillary electrophoresis with inductively coupled plasma-mass spectrometric and electrospray time of flight mass spectrometric detection for the determination of arsenic species in fish samples. Electrophoresis. 2008;29:2731–7.
16. Böhm D, Matysik F-M. Characterization of linearly coupled capillaries with various inner diameters in the context of capillary electrophoresis. Monatsh Chem. 2021;152:1053–60.
17. Tůma P, Opekar F, Samcová E. Very fast electrophoretic separation on commercial instruments using a combination of two capillaries with different internal diameters. Electrophoresis. 2013;34:552–6.
18. Jooß K, Scholz N, Meixner J, Neusüß C. Heart-cut nano-LC-CZE-MS for the characterization of proteins on the intact level. Electrophoresis. 2019;40:1061–5.
19. Sydes D, Kler PA, Hermans M, Huhn C. Zero-dead-volume interfaces for two-dimensional electrophoretic separations. Electrophoresis. 2016;37:3020–4.
20. Pham TTT, Mai TD, Nguyen TD, Sáiz J, Pham HV, Hauser PC. Automated dual capillary electrophoresis system with hydrodynamic injection for the concurrent determination of cations and anions. Anal Chim Acta. 2014;841:77–83.
21. Matysik F-M. Non-aqueous capillary electrophoresis with electrochemical detection. J Chromatogr A. 1998;802:349–54.
22. Riekkola M-L. Recent advances in nonaqueous capillary electrophoresis. Electrophoresis. 2002;23:3865–83.

23. Francisco KJM, do Lago CL. A compact and high-resolution version of a capacitively coupled contactless conductivity detector. Electrophoresis. 2009;30:3458–64.

SUPPORTING INFORMATION

Additional supporting information may be found in the online version of the article at the publisher's website.

How to cite this article: Böhm D, Koall M, Matysik F-M. Dead volume–free flow splitting in capillary electrophoresis. Electrophoresis. 2022;43:1438–1445. https://doi.org/10.1002/elps.202200025